

The Fermi level dependence of the optical and magnetic properties of $\text{Ga}_{1-x}\text{Mn}_x\text{N}$ grown by metal–organic chemical vapour deposition

M Strassburg^{1,2}, M H Kane^{2,3}, A Asghar², Q Song⁴, Z J Zhang⁴,
J Senawiratne¹, M Alevli¹, N Dietz¹, C J Summers³ and I T Ferguson^{2,3}

¹ Georgia State University, Department of Physics and Astronomy, Atlanta, GA 30302-4106, USA

² Georgia Institute of Technology, School of Electrical and Computer Engineering, Atlanta, GA 30332-0250, USA

³ Georgia Institute of Technology, School of Materials Science and Engineering, Atlanta, GA 30332-0245, USA

⁴ Georgia Institute of Technology, School of Chemistry and Biochemistry, Atlanta, GA 30332-0400, USA

E-mail: ianf@ece.gatech.edu

Received 30 June 2005, in final form 25 October 2005

Published 17 February 2006

Online at stacks.iop.org/JPhysCM/18/2615

Abstract

The suppression of the ferromagnetic behaviour of metal–organic chemical vapour deposition grown $\text{Ga}_{1-x}\text{Mn}_x\text{N}$ epilayers by silicon co-doping, and the influence of the Fermi level position on and its correlation with the magnetic and optical properties of $\text{Ga}_{1-x}\text{Mn}_x\text{N}$ are reported. Variation in the position of the Fermi level in the GaN bandgap is achieved by using different Mn concentrations and processing conditions as well as by co-doping with silicon to control the background donor concentration. The effect on Mn incorporation on the formation of defect states and impurity induced energy states within the bandgap of GaN was monitored by means of photoluminescence absorption and emission spectroscopy. A broad absorption detected around 1.5 eV is attributed to the presence of a subband introduced by Mn induced energy states due to temperature independent transition energies and linewidths. The intensity and the linewidth of the absorption band correlate with the Mn concentration. Similarly, the magnitude of the magnetization decreases as the Fermi level approaches the conduction band, as the Fermi energy is increased above the $\text{Mn}(0/-)$ acceptor state. Silicon concentrations $>10^{19} \text{ cm}^{-3}$ caused the complete loss of ferromagnetic behaviour in the epilayer. The absorption band at 1.5 eV is also not observed upon silicon co-doping. The observed spectroscopic data favour a double-exchange-like mechanism rather than an itinerant free carrier mechanism for causing the ferromagnetism. This behaviour significantly differs from the properties reported for widely studied (Ga, In)MnAs.

There has been increased interest in transition metal (TM) doped wide bandgap materials, such as $\text{Ga}_{1-x}\text{Mn}_x\text{N}$, that was triggered by theoretical predictions suggesting that ferromagnetism of diluted magnetic semiconductors with Curie temperatures above room temperature can be obtained [1]. The theoretical work by Dietl *et al* [1] states that the ferromagnetism is facilitated by interaction between the Mn^{2+} ions and holes from the GaN valence band. This assumption suggests that the preparation of p-type material would be required to shift the Fermi level further towards the valence band to increase the observed ferromagnetism [2]. The theory still predicts the observation of ferromagnetism in n-type material but much weaker (more than four times) than that observed in p-type material. Experimental identification of the Mn ion charge state is enabled by electron spin paramagnetic resonance (EPR) and optical spectroscopy [2–5]. The existence of room temperature ferromagnetism in $\text{Ga}_{1-x}\text{Mn}_x\text{N}$ has also been predicted by other theoretical studies which suggest that a Mn induced impurity band provides effective-mass transport within the band [6, 7]. Sato *et al* [7] stated that the incorporation of Mn^{3+} facilitates the formation of a sharp E impurity band and a broader T_2 impurity band, altering the electronic structure in the bandgap of $\text{Ga}_{1-x}\text{Mn}_x\text{N}$. In this model, broadening of the partially filled T_2 band stabilizes the ferromagnetism via the double-exchange interaction [8, 9], provided the Fermi level is located in the defect band. This mechanism differs significantly from that theoretically predicted and experimentally confirmed for $\text{Ga}_{1-x}\text{Mn}_x\text{As}$ [1, 10]. Reed *et al* have recently shown a strong correlation between the observed magnetic signature and the position of the Fermi level in $\text{Ga}_{1-x}\text{Mn}_x\text{N}$ [11]. Further energy states in the GaN bandgap due to the Mn incorporation have been reported from optical spectroscopy causing photoluminescence (PL) bands predominantly in the blue, and in the yellow spectral range [4, 12–15]. However, implantation induced defect states cannot be completely ruled out as a cause for these PL bands, since most of the structures are ion-implanted $\text{Ga}_{1-x}\text{Mn}_x\text{N}$ epilayers. Correlation of these magnetic observations with optical, electronic and structural investigations may improve the fundamental understanding of the nature of the ferromagnetic interaction in these materials.

In this paper, an investigation of the Fermi level dependence and of the magnetization and corresponding optical properties in MOCVD grown $\text{Ga}_{1-x}\text{Mn}_x\text{N}$ is presented. Room temperature ferromagnetism was observed in samples with Mn concentrations between 1 and 2%. The magnitude of the magnetization scaled with the Mn concentration and showed a strong dependence on the position of the Fermi level; additionally, it varied with the silicon co-doping. Complete suppression of the ferromagnetic behaviour was observed upon silicon co-doping to $>10^{19} \text{ cm}^{-3}$. A broad absorption band detected around 1.5 eV is assigned to a Mn induced impurity band and showed a dependence on doping similar to that observed for the magnetization dependence. These experimental findings rather favour a double-exchange-like interaction causing the observed ferromagnetic behaviour in $\text{Ga}_{1-x}\text{Mn}_x\text{N}$, in that variable range hopping between mixed-valence deep level transition metal impurities is likely the source of ferromagnetism. This mechanism is different to that typically reported valence band carrier mediated mechanism for $\text{Ga}_{1-x}\text{Mn}_x\text{As}$ underlining the significant differences between TM doped nitrides and arsenides.

Epitaxial $\text{Ga}_{1-x}\text{Mn}_x\text{N}$ films with Mn concentration up to $\sim 2\%$ were grown on GaN template layers in a specifically modified VEECO D125-MOCVD reactor. Bis-cyclopentadienyl manganese (Cp_2Mn) and silane (SiH_4) were used as the manganese and n dopant sources respectively. A more detailed description of the growth is given elsewhere [16, 17]. Subsequent characterization of these thin films included x-ray diffraction (XRD), secondary-ion mass spectroscopy (SIMS), SQUID magnetometry, photoluminescence (PL) and transmission spectroscopy. The PL was excited by a frequency-doubled titanium–sapphire laser; transmission was effected using the red and infrared spectrum of a halogen lamp. The emitted and transmitted light was detected by a photomultiplier attached to a 0.24 m

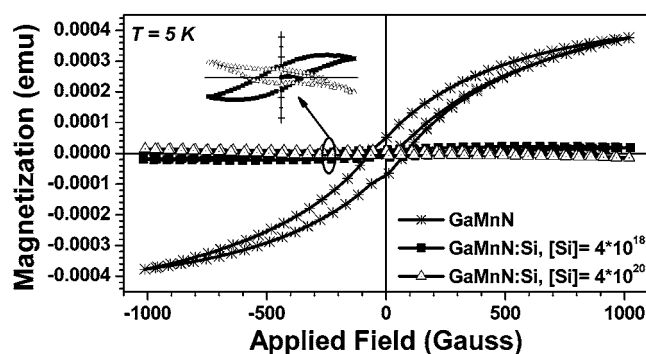


Figure 1. Magnetization spectra of $\text{Ga}_{0.985}\text{Mn}_{0.015}\text{N}$ and $\text{Ga}_{1-x}\text{Mn}_x\text{N}:\text{Si}$ for two different Si concentrations recorded at 5 K. The latter are also shown in the inset on a smaller scale. The observed hysteresis indicates the ferromagnetic behaviour of the Mn doped sample. Upon Si co-doping, the Fermi level shifts towards the bottom of the conduction band, reducing the ferromagnetic interaction. For the highest Si concentration, the ferromagnetic contribution is completely suppressed. The diamagnetic behaviour is due to the sapphire substrate.

monochromator with a spectral resolution of better than 1 nm for emission and better than 6 nm for transmission experiments.

The crystalline quality of $\text{Ga}_{1-x}\text{Mn}_x\text{N}$ and the absence of secondary phases in the layers were confirmed by XRD analysis described in more detail elsewhere [16, 17]. The Mn concentration was varied between 0.3% and 1.5% as confirmed by various techniques. Slight variations in Mn concentrations and thicknesses across the wafer were established on the basis of the gas flow and the temperature gradients in the MOCVD growth. Ferromagnetic behaviour, indicated by hysteresis in the magnetization spectra, was detected in the $\text{Ga}_{1-x}\text{Mn}_x\text{N}$ samples at doping levels of 1.5%, as shown in figure 1. Two significant results were obtained. First, the saturation magnetization (the size of the hysteresis loop) scales with the Mn concentration confirming that Mn doping causes the observed ferromagnetic properties. Hence, mandatory contributions from the Cr^{3+} impurities in the substrate as observed and confirmed by means of EPR for other samples [18] can be ruled out as the primary source of the ferromagnetic behaviour. Secondly, with increasing silicon concentration, the size of the hysteresis loop decreases significantly (by more than one order of magnitude). Although the results are shown at 5 K, the magnetic hysteresis persists and an almost identical magnetization curve is observed at room temperature. The Curie temperature was not measured due to experimental limitations, but there is only a little drop-off in the observed magnetization between 5 and 300 K indicating that T_c is well above room temperature, as reported elsewhere [15]. At high Si concentration ($[\text{Si}] > 10^{19} \text{ cm}^{-3}$), ferromagnetic behaviour is suppressed and the magnetization spectra reveal an overall diamagnetic behaviour for this sample due to the contribution from the sapphire substrate. The suppression is attributed to the shift of the Fermi level towards the conduction band and above the $\text{Mn}^{2+/3+}$ acceptor level, when the Mn acceptors are finally overcompensated by silicon that introduces shallow donor states in GaN. EPR investigations confirm the presence of the Mn^{2+} state for the Si co-doped samples [18]. Si co-doping in GaN normally increases the free carrier concentration providing electrons in the conduction band. According to the Zener mean field model based theories, an increasing n-type carrier concentration would also yield an increase of the magnetization, which was not observed in this work (figure 1). However, it is questionable whether the carrier and Mn concentrations are high enough in this case to render the mean field carrier mediated model applicable. Unlike that

of $\text{Ga}_{1-x}\text{Mn}_x\text{As}$, the magnetization behaviour of $\text{Ga}_{1-x}\text{Mn}_x\text{N}$ can be understood assuming the formation of a partially filled Mn induced band. The ferromagnetism is thus stabilized by the double-exchange-like interaction of electrons in this band. In the case of low concentration Si co-doping, not every Mn acceptor state is compensated. Hence, holes are present in this band; the magnetic ordering in optimally MOCVD grown $\text{Ga}_{1-x}\text{Mn}_x\text{N}$ is attributed to exchange between electrons localized on the levels lying deep in the forbidden energy gap [19]. The reduction of available free states for the double-exchange-like interaction (holes) in the T_2 band holds for the observed smaller magnetization [7].

The measured carrier type in all of these samples is n type in all cases, similar to what has been reported for ferromagnetic $\text{Ga}_{1-x}\text{Mn}_x\text{N}$ in the literature [20]. However, it is likely that this is merely a function of the template layer used to grow the samples, especially in the samples without Si co-doping. To achieve high structural quality for the $\text{Ga}_{1-x}\text{Mn}_x\text{N}$ layer, these epilayers were grown on 1 μm thick GaN template layers; for the Si co-doped samples, these layers were doped n type. The measured Hall concentrations of the as-grown, unintentionally doped $\text{Ga}_{1-x}\text{Mn}_x\text{N}$ films were around $n = 5 \times 10^{16} \text{ cm}^{-3}$, which is very close to the measured background carrier concentration of the unintentionally doped template layer. Similarly increasing the Si doping within the $\text{Ga}_{1-x}\text{Mn}_x\text{N}$ layer does not result in an increase in measured carrier concentration from the $n = 8 \times 10^{17} \text{ cm}^{-3}$ that was almost exactly the measured carrier concentration in the n-type template layer on which these samples were grown. Thus, all of the measured n-type behaviour is due to parallel conduction through the virtual template, and the observed 'n-type' character that is often reported in these systems may be solely due to the template. In order to clarify this point, layers were grown from the substrate with Mn in the virtual template layers. For these samples, the resistivity was too high to measure and the contact resistance increased by several orders of magnitude, consistent with predictions and other observation of Mn as a deep impurity level. It should be noted that the layer grown on the Mn-containing template has a reduced quality and does not exhibit strong ferromagnetism even though it exhibits a strong reddish tint indicative of Mn^{2+} incorporation.

To check whether the magnetic behaviour is due to second phases or clusters, the concentration per magnetic element was calculated. Assuming a uniform growth rate and Mn concentration as measured using SIMS across the wafer, the measured saturation magnetization corresponds to a contribution of $2.9 \mu_B/\text{Mn}$ for the 1% doped sample and $1.2 \mu_B/\text{Mn}$ for the 1.5% doped sample. This compares favourably with the predicted contribution based on first-principles band structure calculations of $4 \mu_B/\text{Mn}$ when the Fermi level is located in the centre of the Mn impurity band [6, 21]. The predicted contributions for the mean field model are also around $4 \mu_B/\text{Mn}$ for hole mediated ferromagnetism, though experimentally for $\text{Ga}_{1-x}\text{Mn}_x\text{As}$ these values are often much lower than anticipated especially at high doping levels due to defect cluster and/or defect compensation [22]. For comparison, the predicted magnetic moment per Mn_4N cluster is $17 \mu_B/\text{Mn}$ [23]. Thus, if the ferromagnetism was due only to this atomic configuration, more than half of the Mn would have been tied up in these clusters, which should be observable through structural characterization techniques. However, since a phase separation based FM has been observed in ferromagnetic chalcopyrite materials with similar magnetization strength, further work is required to unambiguously rule out clusters as the origin of FM in MOCVD grown $\text{Ga}_{1-x}\text{Mn}_x\text{N}$ [24, 25].

To clarify whether isolated Mn ions (as observed for bulk $\text{Ga}_{1-x}\text{Mn}_x\text{N}$ [26] and $\text{Ga}_{1-x}\text{Mn}_x\text{As}$) or the formation of an Mn induced impurity energy band [6, 7] are the primary cause for the observed ferromagnetism, transmission and PL emission studies were performed. The transmission spectra of four samples are shown in figure 2. Both the Mn content and/or the donor concentration were varied during the MOCVD growth. The latter was predominantly achieved by Si co-doping during the growth. Despite high Si concentrations,

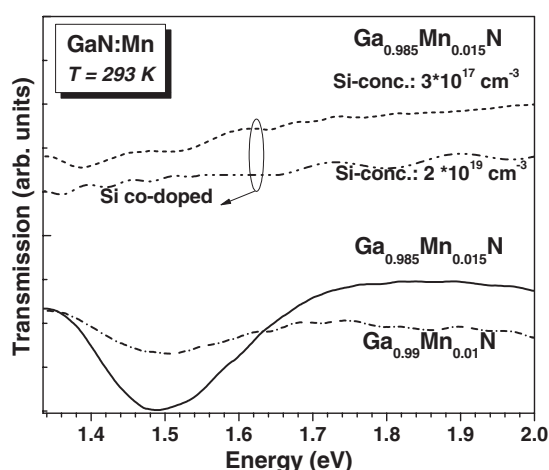


Figure 2. Transmission spectra of $\text{Ga}_{1-x}\text{Mn}_x\text{N}$ and $\text{Ga}_{1-x}\text{Mn}_x\text{N}:\text{Si}$ with varying Mn and Si concentrations. An absorption band around 1.5 eV is detected, but not upon Si co-doping. The intensity and the halfwidth (FWHM) of the absorption band increase with increasing Mn concentration. The spectra of the Si co-doped samples are shifted vertically for clarity.

Hall measurements showed only a slight increase in free electron density in the conduction band, due to trapping of the Si donor electrons by the deeper Mn states. The optical analysis suggests that the incorporation of Mn into the GaN layers during growth leads to an absorption band (dip in transition spectra) around 1.5 eV. This energy is attributed to the transitions from the T_2 states to the E states of the 5D level of the Mn^{3+} ion in the GaN environment [2]. Internal atomic transitions in isolated Mn ions were ruled out due to the relatively large linewidth (full width at half-maximum—FWHM) of 120 meV for this absorption band. The intensity and linewidth of this band scale with the Mn concentration; the absorption depth (FWHM of the absorption band near 1.4 eV) is 1.8% (120 meV) for the 1% Mn sample, and 6.0% (180 meV) for the 1.5% Mn sample. This absorption peak is not observed for nominally undoped GaN grown on sapphire (not shown here) and $\text{Ga}_{1-x}\text{Mn}_x\text{N}$ layers co-doped with silicon corresponding to a strong sensitivity to the position of the Fermi level. As mentioned above, silicon introduces shallow donor states in GaN, which leads to a partial or full compensation of the acceptor states introduced by the Mn ions. Hence, electrons are trapped at deep defects and the position of the Fermi level shifts towards the conduction band. No further absorption features were found in the infrared spectral range down to 0.5 eV. These findings indicate that the Fermi level in the samples investigated in the broad absorption band is located around 1.8 eV above the valence band energy or even closer to the conduction band. Moreover it shows that the cause of the ferromagnetism is significantly different from the mechanisms observed in $\text{Ga}_{1-x}\text{Mn}_x\text{As}$.

Further information about the origin of the observed absorption band was derived from temperature dependent absorption measurements. Variations in the absorption position and linewidth of the band are expected if intra-atomic transitions of isolated Mn ions cause the absorption. However, no significant changes in the shape and transition energy in this energy band were observed on varying the temperatures between 6 and 300 K (see figure 3). All samples have shown Fabry–Perot (FP) interference patterns. This is due to the epilayer thickness providing standing wave conditions for the sapphire/GaN interface and the GaMnN/air interface. Hence the layer thickness is $\sim 2 \mu\text{m}$, which is consistent with *in situ*

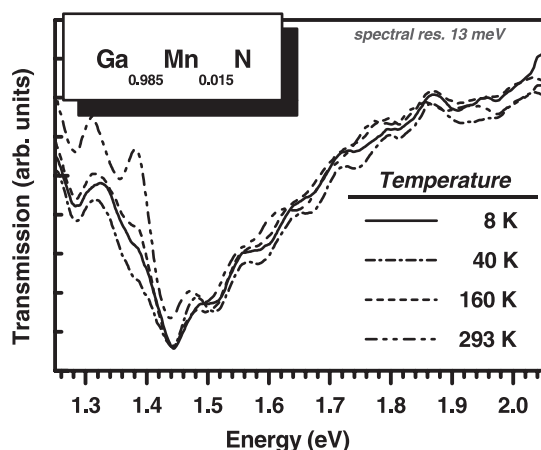


Figure 3. Transmission spectra of $\text{Ga}_{0.985}\text{Mn}_{0.015}\text{N}$ (the sample with the highest Mn concentration) recorded between 8 and 293 K. Both, the position and the halfwidth (FWHM) of the absorption band (dip in the transmission spectra) are independent of the temperature.

monitoring of the reflectivity during the MOCVD growth of these films. This interference pattern was more pronounced in the case of the temperature dependent measurement due to the measurement conditions. A narrowing of the transition bands was not observed (FWHM between ~ 165 and 200 meV; compare to 180 meV at RT), superimposed with the FP effect. In addition, although II–VI compounds are known to have strong electron–phonon couplings, recent infrared transmission measurements performed on MBE grown material suggest that the electron–phonon coupling in $\text{Ga}_{1-x}\text{Mn}_x\text{N}$ is relatively weak [27], although the superposition of phonon replicas in the absorption data presented here has not been eliminated. These findings support the observations that disorder induced broadening in the partially filled T_2 band can be linked to the observed transition.

Additional PL studies were performed in the visible spectral range in order to derive more information on the ferromagnetic nature and Mn induced disorder of $\text{Ga}_{1-x}\text{Mn}_x\text{N}$ layers. The PL data for epitaxially grown GaMnN are shown in figure 4. The blue emission band was found to govern the PL spectrum of the samples with a Mn concentration of $>0.5\%$, resulting in two distinct peaks at 3.0 and 2.8 eV. These bands are also known to appear in GaN upon compensation of acceptors by doping induced defect states as well as by the incorporation of hydrogen on interstitial sites. Accordingly, heavy Mn doping, in particular the band at 3.0 eV, is attributed to Mn induced transitions. Recently, the blue band emission was observed in MBE grown $\text{Ga}_{1-x}\text{Mn}_x\text{N}$ and ion-implanted material [15], and the appearance of these bands, actually a broad emission consisting of several bands (>7 distinct bands) ranging from 2.7 to 3.1 eV, was assigned to transitions from conduction band electrons to Mn related states and from shallow donors (e.g., N vacancies) to Mn acceptor states [12–15]. In contrast, nearly no blue band emission was present, but a pronounced yellow band attributed to intrinsic gallium defects was observed in the lightly doped $\text{Ga}_{1-x}\text{Mn}_x\text{N}$ samples ($<0.5\%$) described elsewhere [16, 17]. This behaviour is a direct consequence of the lower amount of Mn ions available to substitute on lattice sites, reducing the amount of Ga vacancies. This is in agreement with the reduced intensity of the absorption band around 1.5 eV. A similar correlation is found for decreasing Mn concentration in $\text{Ga}_{1-x}\text{Mn}_x\text{N}$. A stronger compensation of Mn acceptors is seen for Si co-doping. Its PL is similar to that detected for $\text{Ga}_{1-x}\text{Mn}_x\text{N}$ with low Mn concentration, underlining that the origin of these particular blue bands observed here can be assigned to

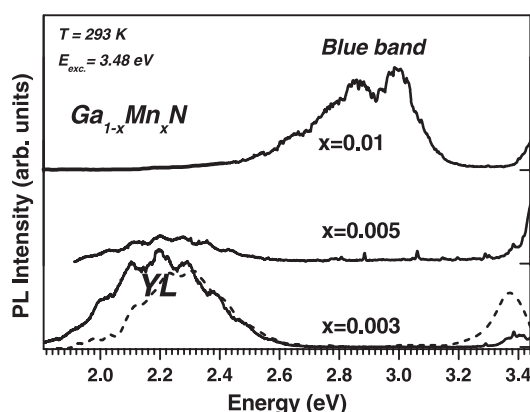


Figure 4. Photoluminescence of GaMnN recorded in the visible and UV spectral range. Higher Mn incorporation led to the appearance of a blue emission band around 3.0 eV. Meanwhile the intensity of the yellow band was reduced. For comparison, the PL of a $\text{Ga}_{0.985}\text{Mn}_{0.015}\text{N}:\text{Si}$ sample is shown (dashed line).

(active) Mn acceptor related states as described above [12–15]. Hence, no emission around 3.0 eV was observed in compensated or partly compensated material.

In conclusion, it has been demonstrated that the observation of ferromagnetism in MOCVD grown $\text{Ga}_{1-x}\text{Mn}_x\text{N}$ is strongly correlated with the position of the Fermi level. Co-doping with silicon facilitated the filling of the partially filled T_2 states compensating the neutral Mn acceptor states. Hence, the Fermi level shifts towards the conduction band. It was found that the double-exchange-like hopping interaction most probably causes the ferromagnetism in MOCVD grown $\text{Ga}_{1-x}\text{Mn}_x\text{N}$, which is significantly different from the $\text{Ga}_{1-x}\text{Mn}_x\text{As}$ case. The strongest magnetization per incorporated Mn was recorded for $\text{Ga}_{0.99}\text{Mn}_{0.01}\text{N}$ epilayers, while a decrease in magnetization per Mn was observed for larger Mn concentration and was found to become even more significant with increasing Si concentration. Two features detected in absorption and PL spectra are correlated with the magnetization of MOCVD grown $\text{Ga}_{1-x}\text{Mn}_x\text{N}$ epilayers. The presence of a blue emission around 3.0 eV as well as an absorption band around 1.5 eV are assigned to the incorporation of Mn ions. The latter is attributed to a disorder induced broadening in the partially filled T_2 band of Mn^{3+} ions in GaN that is known to stabilize ferromagnetism.

Acknowledgments

The authors are grateful to Professor W Gehlhoff from Technical University Berlin, Germany, for EPR expertise and fruitful discussions. MS gratefully acknowledges the support from the Alexander von Humboldt Foundation. MHK was supported by the United States Department of Defense. This work was supported in part by grants from the National Science Foundation (ECS#0224266, U Varshney) and Air Force Office of Scientific Research (T Steiner).

References

- [1] Dietl T, Ohno H, Matsukura F, Cibert J and Ferrand D 2000 *Science* **287** 1019
- [2] Graf T, Gjukic M, Brandt M S, Stutzmann M and Ambacher O 2002 *Appl. Phys. Lett.* **81** 5159
- [3] Baranov P G, Ilyin I V, Mokhov E N and Roenkov A D 1996 *Semicond. Sci. Technol.* **11** 1843

- [4] Korotkov R Y, Gregie J M and Wessels B W 2002 *Appl. Phys. Lett.* **80** 1731
- [5] Gelhausen O, Malguth E, Phillips M R, Goldys E M, Strassburg M, Hoffmann A, Graf T, Gjukic M and Stutzmann M 2004 *Appl. Phys. Lett.* **84** 4514
- [6] Kronik L, Jain M and Chelikowsky J R 2002 *Phys. Rev. B* **66** 041203
- [7] Sato K, Dederichs P H, Katayama-Yoshida H and Kudrnovsky J 2003 *Physica B* **340–342** 863
- [8] Akai H 1998 *Phys. Rev. Lett.* **81** 3002
- [9] Sato K and Katayama-Yoshida H 2002 *Semicond. Sci. Technol.* **17** 367
- [10] Kudrnovsky J, Drchal V, Turek I, Bergqvist L, Eriksson O, Bouzerar G, Sandratskii L and Bruno P 2004 *J. Phys.: Condens. Matter* **16** S5571
- [11] Reed M J, Arkun F E, Berkman E A, Elmasry N A, Zavada J, Luen M O, Reed M L and Bedair S M 2005 *Appl. Phys. Lett.* **86** 102504
- [12] Shon Y, Hae K Y, Yuldashev Sh U, Leem J H, Park C S, Fu D J, Kim H J, Kang T W and Fan X J 2002 *Appl. Phys. Lett.* **81** 1845
Shon Y, Hae K Y, Yuldashev Sh U, Park Y S, Fu D J, Kim D Y, Kim H S and Kang T W 2003 *J. Appl. Phys.* **93** 1546
- [13] Xu J, Li J, Zhang R, Xiu X Q, Lu D Q, Gu S L, Shen B, Shi Y and Zheng Y D 2002 *Mater. Res. Soc. Symp. Proc.* **693** 207
- [14] Polyakov A Y, Smirnov N B, Govorkov A V, Pashkova N Y, Kim J, Ren F, Overberg M E, Thaler G T, Abernathy C R, Pearton S J and Wilson R G 2002 *J. Appl. Phys.* **92** 3130
- [15] Baik J M, Lee J-L, Shon Y and Kang T W 2003 *J. Appl. Phys.* **93** 9024
- [16] Kane M H, Asghar A, Payne A M, Vestal C R, Strassburg M, Senawiratne J, Zhang Z J, Dietz N, Summers C H and Ferguson I T 2005 *Semicond. Sci. Technol.* **20** L5
- [17] Kane M H, Asghar A, Payne A M, Vestal C R, Zhang Z J, Strassburg M, Senawirante J, Dietz N, Summers C R and Ferguson I T 2005 *Phys. Status Solidi c* **7** 2441
- [18] Gehlhoff W 2005 private communication, TU Berlin, Germany
- [19] Fleurov V, Kikoin K, Ivanov V A, Krstajic P M and Peeters F M 2004 *J. Magn. Magn. Mater.* **272–276** 1967
- [20] Overberg M E, Abernathy C R, Pearton S J, Theodoropoulou N A, McCarthy K T and Hebard A F 2001 *Appl. Phys. Lett.* **79** 1312
- [21] Sanyal B, Bengone O and Mirbt S 2003 *Phys. Rev. B* **68** 205210
- [22] Potashnik S J, Ku K C, Mahendiran R, Chun S H, Wang R F, Samarth N and Schiffer P 2002 *Phys. Rev. B* **66** 012408
- [23] Rao B K and Jena P 2002 *Phys. Rev. Lett.* **89** 185504
- [24] Hwang T, Shim J H and Lee S 2003 *Appl. Phys. Lett.* **83** 1809
- [25] Cho S, Choi S and Cha G-B 2002 *Phys. Rev. Lett.* **88** 257203
- [26] Wolos A, Palczewska M, Zajac M, Gosk J, Kaminska M, Twardowski A, Bockowski M, Grzegory I and Porowski S 2004 *Phys. Rev. B* **69** 115210
- [27] Yamamoto T, Marcet S, Gheeraert E, Kuroda S, Mariette H, Ferrand D and Cibert J 2005 *J. Cryst. Growth* **275** e2233–7